Molecular Crystals and Liquid Crystals

Publication details, including instructions for authors and subscription information:
http://www.tandfonline.com/loi/gmcl20

Stability, Release Property and Skin Penetration of Stearic Acid Nanoparticles

Hyang Hee Joo [a], Hyeon Yong Lee [a] & Jin-Chul Kim [a]

[a] School of Biotechnology & Bioengineering and Institute of Bioscience and Biotechnology, Kangwon National University, Chunchon, Kangwon-do, Korea

Version of record first published: 05 Oct 2009

To cite this article: Hyang Hee Joo, Hyeon Yong Lee & Jin-Chul Kim (2009): Stability, Release Property and Skin Penetration of Stearic Acid Nanoparticles, Molecular Crystals and Liquid Crystals, 508:1, 137/[499]-149/[511]

To link to this article: http://dx.doi.org/10.1080/15421400903060466

Mol. Cryst. Liq. Cryst., Vol. 508, pp. 137/[499]–149/[511], 2009

ISSN: 1542-1406 print/1563-5287 online
DOI: 10.1080/15421400903060466

Stability, Release Property and Skin Penetration of Stearic Acid Nanoparticles

Hyang Hee Joo, Hyeon Yong Lee, and Jin-Chul Kim
School of Biotechnology & Bioengineering and Institute of Bioscience and Biotechnology, Kangwon National University, Chunchon, Kangwon-do, Korea

Stearic acid nanoparticles were prepared by a melt-emulsification method. The nanoparticles were stable in terms of the size and the appearance when the concentrations of sodium lauryl sulfate in the suspensions were less than 1.443%. And, they were stable in the aspect of their integrity when the concentrations of ethanol in the suspensions were less than 20%. For the release and the skin permeation experiment, hinokitiol (HKL) was used as a model drug and it was encapsulated in the nanoparticles. The % release of HKL was observed in distilled water and alcoholic solutions of 5% and 10%. The release increased up to 45%–55% for the first 8 h and thereafter no significant release was observed. According to the results of a confocal laser scanning microscopy, the nanoparticles were found to be in the dermis of a hairless mouse skin. The nanoparticles present in the dermis would act as depots for the dermal delivery of HKL.

Keywords: confocal laser scanning microscopy; nanoparticle; release; stability; stearic acid

1. INTRODUCTION

Drug delivery carriers, such as lipid vesicle, micelle, and nanoparticles have found their applications in the transdermal delivery of biologically active agents. For the dermal delivery of enoxacin [1], diclofenac [2] and vitamin E acetate [3], lipid bilayer vesicles, liposomes, have been extensively employed as a drug carrier. Cationic vesicles

This work was supported by a grant (KRF-2007-314-C00271) from Korea Research Foundation, Republic of Korea.

Address correspondence to Jin-Chul Kim, School of Biotechnology & Bioengineering and Institute of Bioscience and Biotechnology, Kangwon National University, 192-1, Hyoja 2-dong, Chunchon, Kangwon-do 200-701, Korea. E-mail: jinkim@kangwon.ac.kr

composed of stearamidopropyl dimethyl amine and stearic acid were also found to increase the anti-bacterial activity of triclosan [4]. With aid of the cationic vesicles, an increased substantivity of minoxidil was observed in a rinse-off type of hair cleansing product, giving an after-rinsing hair growth promotion [5]. On the other hand, solid lipid nanoparticles (SLN) have been turned out to be a versatile carrier. The nanoparticles were reported to accommodate triptolide, an anti-inflammatory agent, and enhance the transdermal delivery of the drug [6,7]. It was also evaluated as a vector for a gene delivery. Following the results, it boosted *in vitro* transfection activity by optimizing the cationic lipid and matrix lipid composition of SLN [8]. In addition, a marked reduction in the *in vitro* toxicity of all-*trans* retinoic acid was observed with SLN, while the antiproliferative effects against a wide range of cancer cell lines was kept [9]. Furthermore, the chemotherapeutic potential of orally administered rifampicin, isoniazid and pyrazinamide against experimental tuberculosis was evaluated when they were incorporated in SLN. The anti cancer drugs incorporated in SLNs were much more effective than free ones in terms of extermination of tubercle bacilli [10].

In this study, stearic acid (SA) nanoparticles containing hinokitiol (HKL) were prepared by a melt-emulsification method. Owing to the antimicrobial activity and the inhibitory action on the apoptosis of keratinocyte, much attention is recently paid to the use of HKL as a hair growth promotion agent [11,12]. In order to apply the SLN to cosmetic preparations, it should be robust and stable in surfactant or alcoholic solutions. The use of SLN in cosmetic preparations, however, could be limited due to the solubilization in the solutions. Accordingly, the stabilities against sodium lauryl sulfate (SLS), a detergent, and ethanol were investigated. In parallel, the release behaviors are also important to design the composition of cosmetic vehicles. Accordingly, the degree of release of HKL from the SLN was investigated in alcoholic solution. Another property SLN should have for the cosmetic applications is its penetration into skins. To evaluate the feasibility of the cosmetic application, the *in vitro* skin penetration of the nanoparticles was investigated on a confocal laser scanning microscope.

2. EXPERIMENTAL SECTION

2.1. Materials

Stearic acid (SA) and fluorescein isothiocyanate (FITC) were purchased from Fluka. Hinokitiol (HKL) was provided by LG household and Healthcare (Daejon, South Korea). Cellulose ester membrane

(MWCO 10,000, Dia. 20 mm) for a release test was purchased from Spectrum (Rancho Dominguez, CA). Sodium lauryl sulfate (SLS) was obtained from Sigma. All other reagents were in analytical grade.

2.2. Animals

Female hairless mice (type SKH) were obtained from Orient Bio (Seongnam, South Korea). They were housed in suspended wire mesh cages in a room illuminated from 09:00 to 21:00 h and kept 20–25°C, with a rodent diet and water ad libitum.

2.3. Preparation of Nanoparticles Containing HKL

Stearic acid, 4.0 g, and HKL, 1.2 g, are molten together around 85°C in a beaker of 20 ml. When fluorescence-labeled nanoparticles were prepared, 20 mg of FITC was added to the melt. In parallel, an aqueous solution of Tween 20, 80 ml (2.0%), was prepared in a beaker of 200 ml and then it was heated up to the same temperature. While homogenizing the heated solution, the melt was slowly added to the solution. To obtain an oil-in-water emulsion, the homogenization was kept for 20 min around 85°C. To solidify the oil droplets, the hot emulsion was carefully added to 267 ml of distilled ice water (0°C–5°C).

2.4. Turbidity Measurement of Lipid Colloids with Concentration of SLS and Ethanol

The stabilities of lipid nanoparticles against SLS and ethanol were investigated by observing the change in turbidity of the colloidal dispersion with the concentration of SLS and ethanol. The detergent was added to the nanoparticle suspensions so that the concentrations are from 0% to 17.5% and then they were mixed on a vortex mixer for 1 min. In case of ethanol, the concentration was varied from 0% to 90%. The turbidity was measured at 630 nm on a UV spectrophotometer (JENWAY 6505, UK) 1 h after mixing the suspensions.

2.5. Transmission Electron Microscopy

The nanoparticle suspensions were negatively stained using a phosphotungstic acid solution (2%, pH 6.8) and then it was transferred onto a formvar- and carbon-coated copper grid. After drying the replica at room temperature, the image was observed on a transmission electron microscope (LEO-912AB OMEGA).

2.6. Solubility of HKL in Alcoholic Solution

An excess amount of HKL was added to alcoholic solutions of various concentrations (0%–30%), and they were extensively stirred for 12 h. The suspension was filtered through a syringe filter with pore size of 0.22 μm. The absorbance of filtrate was measured at 370 nm on a UV spectrophotometer (JENWAY 6505, UK) and the solubility was determined by comparing the absorbance with a calibration curve ($A = 244.5 \times C - 0.0064$ with $R^2 = 0.999$, where A is absorbance and C is the concentration of HKL in g/ml).

2.7. Release of HKL from Nanoparticles in Alcoholic Solutions

Ethanol was added to the vigorously stirred colloidal suspensions of HKL-loaded nanoparticles so that the concentrations of the alcohol in the suspensions are 0%, 5%, and 10%. The solid contents (lipid + HKL) in the three suspensions were 0.43 mg/ml, 1.30 mg/ml and 1.73 mg/ml, and the concentrations of HKL in the suspensions were 0.1 mg/ml, 0.3 mg/ml, and 0.4 mg/ml, respectively. And then, each suspension of 10 ml was put into a hydrated dialysis bag and it was dialyzed against 300 ml of an alcoholic solution, of which ethanol concentrations were the same as those of the three suspensions. 1 ml of the dialysis medium was taken at predetermined time intervals and the amount of HKL released was determined by measuring the absorbance of the medium at 370 nm on a UV spectrophotometer (JENWAY 6505, UK). Every time the dialysis medium was taken away, an alcoholic solution of 1 ml was added to compensate for the reduced amount of the dialysis medium. The % release of HKL was determined as follows.

$$\% \text{ Release} = \left(\frac{H_f}{H_t}\right) \times 100$$

Where H_t is the total amount of HKL entrapped in the nanoparticles and H_f is the amount of HKL detected in the dialysis medium at a predetermined time.

2.8. Penetration of Nanoparticles Observed on a Confocal Laser Scanning Microscope

Female hairless mice (type SKH) aged 6 weeks were sacrificed by cervical dislocation. The dorsal skin of each hairless mouse was excised and the adhering fat and other visceral tissue were removed. The skin was mounted onto Franz diffusion cell (0.636 cm^2 surface

area). In order to protect the dehydration of the skin, phosphate buffered saline (PBS, pH 7.4) was used as the receptor content, thermostated at 37°C. 200 μl of fluorescence-labeled nanoparticle suspension was applied onto the skin. 24 h later, the skin was carefully removed from the diffusion cell and the surface was washed three times with distilled water. The washed skin was frozen, and it was vertically sliced using a cryo-microtome (Leica CM 1850) so that the thickness of the sliced skins is 200–220 μm. The cross section was observed at 488 nm on a confocal laser scanning microscope (Olympus LX70 FV300 05-LPG-193).

3. RESULTS AND DISCUSSION

3.1. Integrity of Lipid Nanoparticles with Concentration of SLS and Ethanol

To investigate the integrity of the nanoparticles in the surfactant solutions, the colloid exposed to SLS was investigated on TEM. As shown in Figure 1, the nanoparticles were observed as white domains since the sample were pretreated by a negative staining technique. Phosphotungstic acid, a heavy metal for the staining, is water-soluble and it would stain the area where nanoparticles do not occupy, because SA, comprising the matrix of the nanoparticle, is hydrophobic. Accordingly, electron beams go through the area where the nanoparticles are. However the beams can not pass through the areas where the heavy metals are. Therefore, the black and white contrasts were observed. The nanoparticles obviously survived at lower concentrations of SLS concentration such as 0.029% (Fig. 1a), and no significant changes in the size and the appearance were observed. SLS is an anionic detergent having a strong surface activity and the critical micelle concentration (CMC) is 0.236%. The concentration of 0.029%, however, is far below the CMC. Thus, the action of the detergency would be weak, having little effect on the integrity of the nanoparticles. When the concentration increased up to 0.722% (Fig. 1b) and 1.443% (Fig. 1c), which are above CMC, the shapes were somewhat distorted and larger particles were observed. The hydrophobic hydrocarbon of the detergent could incorporate into the matrix of SA nanoparticles and disturb the crystal structure. Accordingly, the fluidization of the solid matrix of the nanoparticles would occur, leading to the fusion of the fluidic nanoparticles. This may account for the distorted shape and the increased size. In fact, according to a previous report, the turbidity of the colloid increased with SLS concentration in the range of 0%–1.443% [13]. The increased turbidity would be due to the distorted appearance

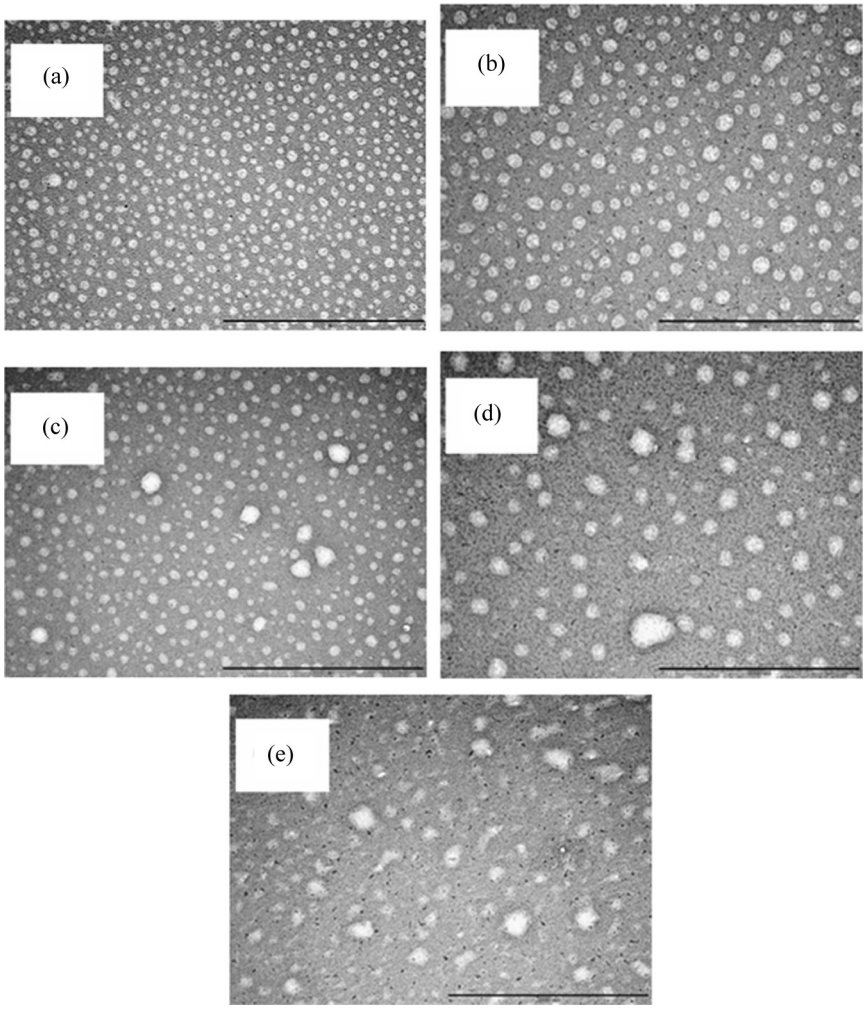

FIGURE 1 Integrity of SA nanoparticles containing HKL in surfactant solutions, observed on TEM. Bars represent 2,000 nm. SLS concentration: (a) 0.0286%; (b) 0.7215%; (c) 1.443%; (d) 2.1645%; (e) 2.886%.

and the increased size. On the other hand, at higher concentrations of SLS such as 2.165% (Fig. 1d) and 2.886% (Fig. 1e), the degree of distortion was outstanding and the size increased much more. However, it was reported that the turbidity decreased with SLS concentration in the higher range (1.443%–2.886%) [13]. Two conflicting findings mean that the solubilization and the fusion seem to occur

simultaneously but the former is prevailing in the higher concentration range. When the concentration was higher than 2.886%, no trace of the nanoparticles was observed. This is due to the complete solubilization of the nanoparticles. At the concentrations higher than 2.886%, the values of the turbidity were almost zero [13].

Figure 2 shows the turbidity variation of SA nanoparticles with ethanol concentration. No marked decrease in the turbidity was observed until the concentration of the alcohol reached 60%. This means that SA is sparely soluble in the alcoholic solutions of which the concentrations are less than 60%. A marked decrease in the turbidity was observed around the concentration and transparent solutions, of which the turbidity were almost zero, were obtained when the concentration of ethanol was more than 60%. This is possibly because SA is readily soluble at the higher concentrations of ethanol and accordingly the nanoparticles are solubilized. In parallel, the integrity of the nanoparticles in the alcoholic solutions was investigated on TEM. As shown in Figure 3, the nanoparticles were obviously found at lower concentrations of alcoholic solution such as 10% (Fig. 3a) and 20% (Fig. 3b), but the spherical shape was rather

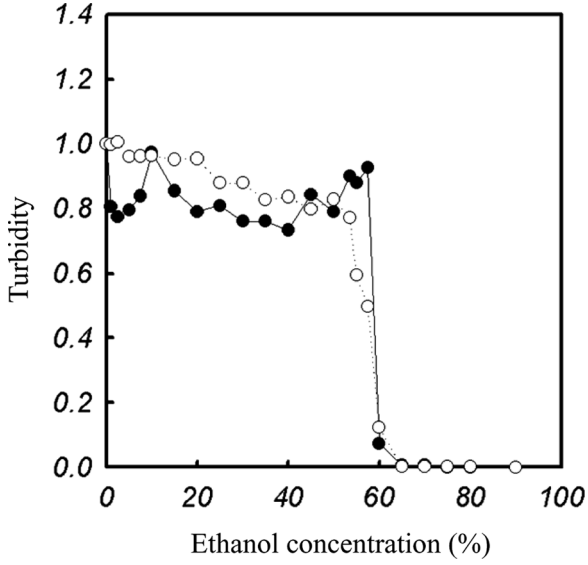

FIGURE 2 Turbidity variations of SA nanoparticles with ethanol concentration. The data are mean values obtained from triplicate experiments and the standard deviations of all the data points fall within 3.0%. Free of HKL (○), Containing HKL (●).

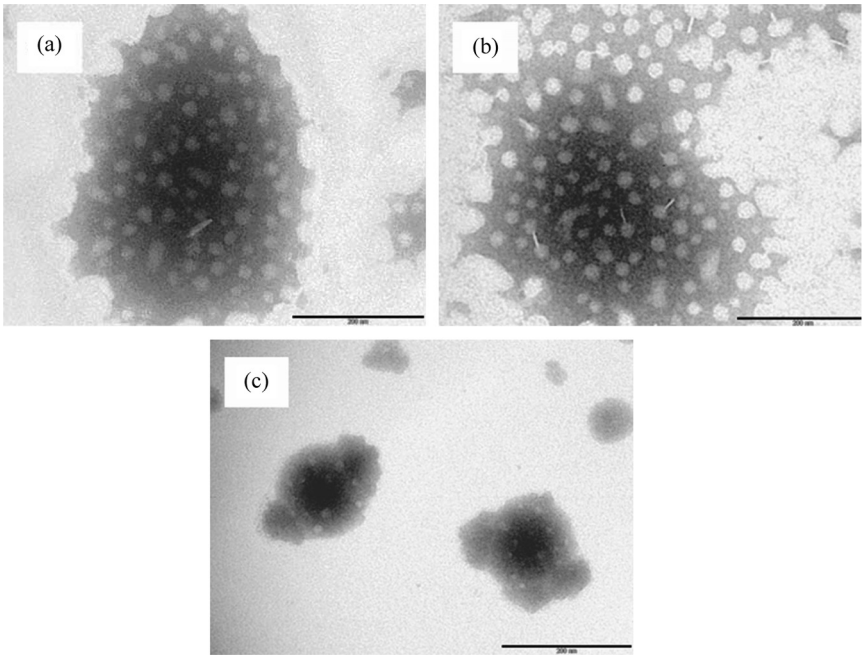

FIGURE 3 Integrity of SA nanoparticles containing HKL in alcoholic solutions, observed on TEM. Bars represent 200 nm. Ethanol concentration: (a) 10%; (b) 20%; (c) 30%.

deformed and some were fused. In the alcoholic solutions, the fatty acids comprising nanoparticles are likely to be partially leached out and the solid nanoparticles could be fluidized. In this circumstance, the nanoparticles would be deformed and fused each other during the dry process for TEM observation. On the other hand, no spherical particle was observed when the nanoparticles were in the alcoholic solutions, of which ethanol concentration were 30% (Fig. 3c), 40% and 50%. According to the results of ethanol concentration-dependent turbidity, however, the turbidities of the suspensions were maintained in the concentration range of 0%–50% (Fig. 2). Considering both the results of TEM and those of turbidity measurements, the spherical nanoparticles were disintegrated into other types of particles, which may be smaller than the solid nanoparticles but large enough to scatter visible lights. In summary, in terms of the size and the appearance, the nanoparticles were robust at SLS concentrations less than 1.443%, and they were stable at ethanol concentration less than 20%.

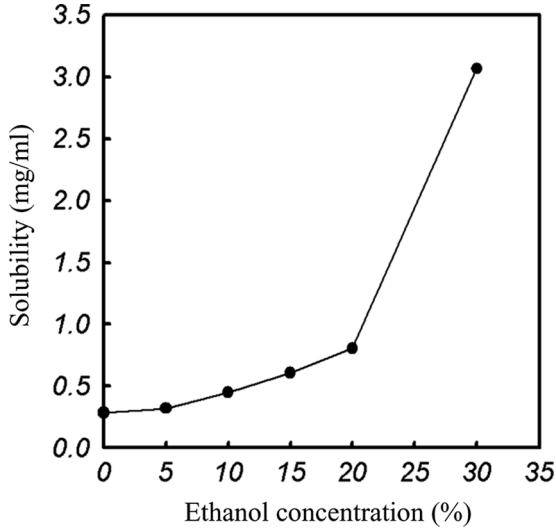

FIGURE 4 Solubility of HKL in alcoholic solutions. The data are mean values obtained from triplicate experiments and the standard deviations of all the data points fall within 1.0%.

3.2. Solubility of HKL in Alcoholic Solution

Figure 4 shows the solubility of HKL in alcoholic solutions. The values exponentially increased, when the concentration of ethanol increased. The solubilities in the alcoholic solutions of 0%, 5%, 10%, 15%, 20% and 30% were 0.283 mg/ml, 0.321 mg/ml, 0.449 mg/ml, 0.607 mg/ml, 0.804 mg/ml and 3.069 mg/ml, respectively. HKL (2-hydroxy-4-isopropyl-2, 4, 6-cyclohepta-2, 4, 6-trine-1-one) is obtained from the essential oils of several kinds of trees. Since it has non-polar seven-membered aromatic ring, the increased solubility was observed in the alcoholic solutions. HKL is reported to be soluble in organic solvents such as ethanol and ether.

3.3. Release of HKL from Nanoparticles in Alcoholic Solutions

Figure 5 shows the % release of HKL from lipid nanoparticles in distilled water and alcoholic solutions. The HLK released in a saturation manner. That is, the release increased up to 45%–55% in 8 h, and thereafter no release was observed. According to the solubility data of HKL (Fig. 4), the concentration of 0.3 mg/ml is a concentration slightly greater than the solubility of HKL in distilled water, 0.283 mg/ml, and it is less than the solubility in 5% alcoholic

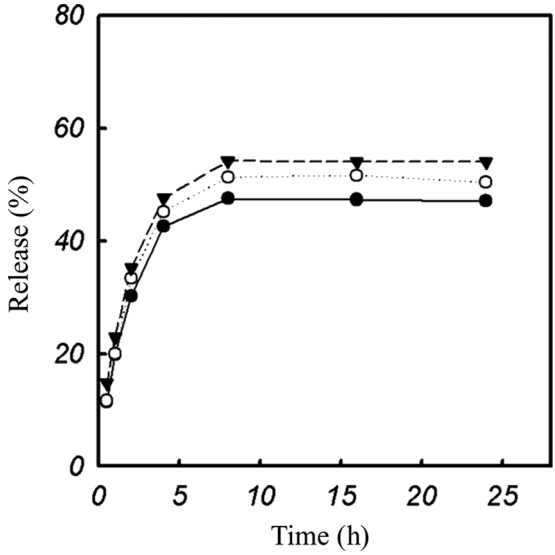

FIGURE 5 Release of HKL from nanoparticles in distilled water and alcoholic solutions. HKL concentration in release medium was 0.3%. The data are mean values obtained from triplicate experiments, and the standard deviations of all the data points fall within 4.0%. The concentrations of ethanol in release media are 0% (●), 5% (○), 10% (▼).

solution, 0.321 mg/ml, and the solubility in 10% alcoholic solution, 0.449 mg/ml. This means that the release was not restricted by the limit of the solubility in the alcoholic solutions. Nevertheless, the maximum % of releases were far below 100%, whether the media are distilled or alcoholic solutions. This is possibly because that HKL is partitioned between the lipid matrix of nanoparticles and the release medium. The maximum% of releases in the alcoholic solutions was higher than in distilled water. Since HKL is more soluble in alcoholic solution than in water, HKL is more readily portioned into release medium of alcoholic solution. This would account for the higher % of release in alcoholic solutions.

Figure 6 shows the effect of HKL concentrations on the % release of HKL in alcoholic solution of 5%. For 4 h, the % release was higher when the concentration of HKL was lower. The HKL concentration of 0.1 mg/ml is a value much less than the solubility of HKL in 5% alcoholic solution, 0.321 mg/ml. The prominent difference between the concentration and the solubility could explain the higher degree of release. On the other hand, the concentrations of 0.3 mg/ml and 0.4 mg/ml are around the solubility of HKL in 5% alcoholic solution.

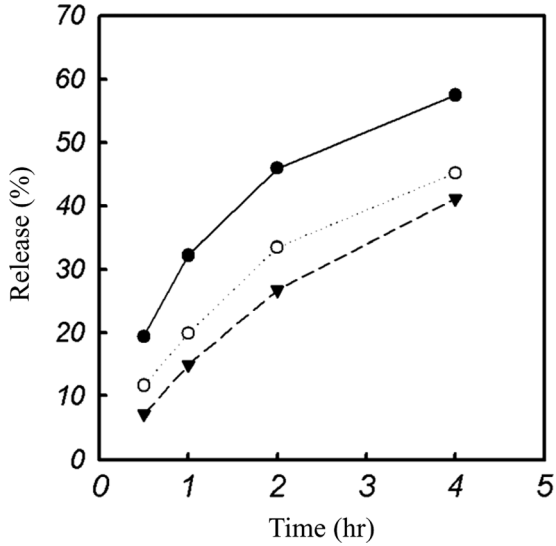

FIGURE 6 Release of HKL from nanoparticles in alcoholic solution of 5%. The data are mean values obtained from triplicate experiments and the standard deviations of all the data points fall within 4.0%. The concentrations of HKL in the alcoholic solution are 0.1 mg/ml (•), 0.3 mg/ml (○), 0.4 mg/ml (▼).

The small difference may account for why the % releases were lower at the higher concentrations of HKL.

3.4. Penetration of Nanoparticles Observed on a Confocal Laser Scanning Microscope

Figure 7 shows the images of fluorescent nanoparticles permeated into a hairless mouse skin, observed on a confocal laser scanning microscope. An intensive fluorescence was observed in the utmost layer (the stratum corneum and the epidermis). During the application period (for 24 h), the fluorescent nanoparticles could penetrate into the stratum corneum and the epidermis, or FITC from the nanoparticles could diffuse into them. The intensity of the fluorescence was so strong that the fluorescent nanoparticles could not be assured to be present in the utmost layer. In the dermis, the nanoparticles were obviously found as fluorescent dots. They were evenly distributed in the upper half of the skin but hardly found in the lower half. According to the results of *in vitro* skin permeation study, SA nanoparticles effectively enhanced the permeability of HKL, compared with other vehicles such as ethanol and propylene glycol [13]. These results mean that the

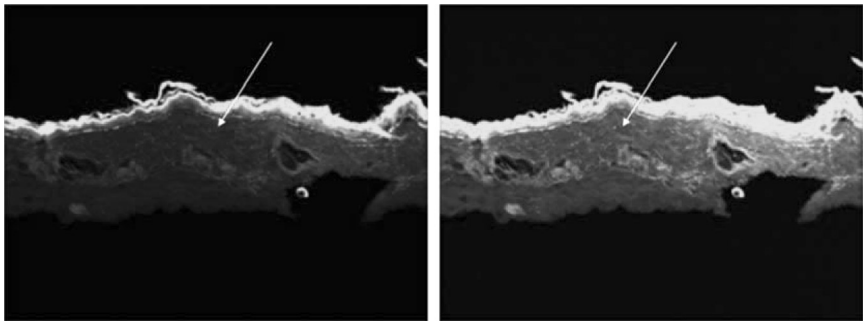

FIGURE 7 Penetration of fluorescent SA nanoparticle containing HKL, observed by confocal laser scanning microscopy. Arrows indicate fluorescent nanoparticles.

enhanced permeability of HKL is not because the nanoparticles pass through the whole skin. Instead, the nanoparticles present in the skins are thought to act as depots of HKL. It is reported that nanoparticles less than 50–100 nm penetrate into hairless mouse skins [14]. Furthermore, when porcine skin was employed in the skin permeation study, even microparticles of several microns were found even in the dermis 24 h after applying them onto the porcine skin [15]. A similar result was obtained by Rolland et al. with porcine skin and microparticles [16]. Since the porcine skin is hairy and the follicular duct is tens of microns, the follicles were thought to be path ways for the penetration of the microparticles. SA nanoparticles prepared in this study was quite mono-dispersive in terms of size and more than 95% of the particles were observed between 35 nm and 51 nm. Due to the small size, the SA nanoparticles would readily penetrate into hairless mouse skins, as observed in Figure 7.

4. CONCLUSIONS

Stearic acid nanoparticles containing hinokitiol could be applied to cosmetic products containing either sodium lauryl sulfate (less than 1.443%) or ethanol (less than 20%) without loss of their integrity, and they could be depots for delivering the active ingredient to skins.

REFERENCES

[1] Fang, J. Y., Sung, K. C., Lin, H. H., & Fang, C. L. (1999). *J. Control. Rel.*, *60*, 1.
[2] Boinpally, R. R., Zhou, S. L., Poondru, S., Devraj, G., & Jasti, B. R. (2003). *Eur. J. Pharm. Biopharm.*, *56*, 389.

[3] Padamwar, M. N. & Pokharkar, V. B. (2006). *Int. J. Pharm.*, *320*, 37.
[4] Kim, J. C., Song, M. E., Kim, M. J., Lee, E. J., Park, S. K., Rang, M. J., & Ahn, H. J. (2002). *Colloid Surf. B: Biointerfaces*, *26*, 235.
[5] Kim, J. C., Lee, M. H., & Rang, M. J. (2003). *Drug Deliv.*, *10*, 119.
[6] Mei, Z., Chen, H., Weng, T., Yang, Y., & Yang, X. (2003). *Eur. J. Pharm. Biopharm.*, *56*, 189.
[7] Mei, Z., Li, X., Wu, Q., Hu, S., & Yang, X. (2005). *Pharmacol. Res.*, *51*, 345.
[8] Tabatt, K., Sameti, M., Olbrich, C., Muller, R. H., & Lehr, C. M. (2004). *Eur. J. Pharm. Biopharm.*, *57*, 155.
[9] Lim, S. J., Lee, M. K., & Kim, C. K. (2004). *J. Control. Rel.*, *100*, 53.
[10] Pandey, R., Sharma, S., & Khuller, G. K. (2005). *Tuberculosis*, *85*, 415.
[11] Kim, Y. S. (2003). Prevention of hair loss and compositions for hair growth promotion, *Korean Patent* no: 10-2003-0041638.
[12] Song, H. H. (2003). Hair growth promotion agents and a screening method for the agents, *Korean Patent* no: 10-2003-7003542.
[13] Cho, S. M., Lee, H. Y., & Kim, J. C. (2007). *J. Am. Oil Chem. Soc.*, *84*, 859.
[14] Shim, J., Kang, H. S., Park, W. S., Han, S. H., Kim, J., & Chang, I. S. (2004). *J. Control. Rel.*, *97*, 477.
[15] de Jalon, E. G., Blanco-Prieto, M. J., Ygartua, P., & Santoyo, S. (2001). *Int. J. Pharm.*, *226*, 181.
[16] Rolland, A., Wagner, N., Chatelus, A., Shroot, B., & Schaefer, H. (1993). *Pharm. Res.*, *10*, 1738.